

Received: 2020.10.01

Accepted: 2020.12.27

Available online: 2021.01.19

Published: 2021.03.18

# Functional Dissection of CD26 and Its Pharmacological Inhibition by Sitagliptin During Skin Wound Healing

**Authors' Contribution:**

Study Design A  
Data Collection B  
Statistical Analysis C  
Data Interpretation D  
Manuscript Preparation E  
Literature Search F  
Funds Collection G

BCD 1 **Yue Jiang\***  
BCF 1 **Yuan Yao\***  
AF 1 **Jin Li**  
CF 1 **Yanling Wang**  
DE 2 **Jie Cheng**  
ADEG 1 **Yumin Zhu**

1 Jiangsu Key Laboratory of Oral Disease, Nanjing Medical University, Nanjing, Jiangsu, R.R. China  
2 Department of Oral and Maxillofacial Surgery, Affiliated Hospital of Stomatology, Nanjing Medical University, Nanjing, Jiangsu, R.R. China

\* Yue Jiang and Yuan Yao contributed equally to this work

**Corresponding Author:** Yumin Zhu, e-mail: [jjyomi@163.com](mailto:jjyomi@163.com)

**Source of support:** This work was financially supported, in whole or in part, by the National Natural Science Foundation of China (81700947)

**Background:** Skin fibroblasts are primary mediators underlying wound healing and therapeutic targets in scar prevention and treatment. CD26 is a molecular marker to distinguish fibroblast subpopulations and plays an important role in modulating the biological behaviors of dermal fibroblasts and influencing skin wound repair. Therapeutic targeting of specific fibroblast subsets is expected to reduce skin scar formation more efficiently.





**Material/Methods:** Skin burn and excisional wound healing models were surgically established in mice. The expression patterns of CD26 during wound healing were determined by immunohistochemical staining, real-time RT-PCR, and western blot assays. Normal fibroblasts from intact skin (NFs) and fibroblasts in wounds (WFs) were isolated and sorted by fluorescence-activated cell sorting (FACS) into 4 subgroups – CD26<sup>+</sup> NFs, CD26<sup>-</sup> NFs, CD26<sup>+</sup> WFs, and CD26<sup>-</sup> WFs – for comparisons of their capacities of proliferation, migration, and collagen synthesis. Pharmacological inhibition of CD26 by sitagliptin in skin fibroblasts and during wound healing were further assessed both in vitro and in vivo.

**Results:** Increased CD26 expression was observed during skin wound healing in both models. The CD26<sup>+</sup> fibroblasts isolated from wounds had significantly stronger abilities to proliferate, migrate, and synthesize collagen than other fibroblast subsets. Sitagliptin treatment potently diminished CD26 expression, impaired the proliferation, migration, and collagen synthesis of fibroblasts in vitro, and diminished scar formation in vivo.

**Conclusions:** Our data reveal that CD26 is functionally involved in skin wound healing by regulating cell proliferation, migration, and collagen synthesis in fibroblasts. Pharmacological inhibition of CD26 by sitagliptin might be a viable strategy to reduce skin scar formation.

**Keywords:** **Dipeptidyl Peptidase 4 • Fibroblasts • Wound Healing • Dipeptidyl-Peptidase IV Inhibitors**

**Full-text PDF:** <https://www.medscimonit.com/abstract/index/idArt/928933>

 3466  —  4  28



## Background

Scar formation, the common result of skin wound healing, seriously impairs the appearance and functions of organs and poses a major health care burden. It is characterized as excessive synthesis, secretion, and abnormal deposition of collagen-dominant extracellular matrix (ECM) [1]. Currently, therapeutic strategies, including hormonal injections, surgical resection, local applications of biological, and lasers, are used in clinical practice to prevent or ameliorate skin scarring [2]. However, these treatments usually fail to achieve optimal effects and do not satisfy the high expectations of patients [3]. Therefore, scar prevention and reduction still are major unresolved challenges in clinical practice.

Skin fibroblasts are the key effector cells involved in wound healing and have strong abilities to synthesize and secrete ECMs to fill wounds and also to differentiate into myofibroblasts for scar contracture [4]. Mounting evidence has suggested that the abundance and functionality of skin fibroblasts often determine the quality and outcomes of wound healing. Therefore, inhibiting excessive collagen synthesis in fibroblasts might effectively reduce skin scar formation. In contrast, enhancing their synthesis of ECM can improve impaired healing in patients with systematic diseases such as diabetes [5,6].

Recently, pioneering studies have revealed that skin fibroblasts are not a unique phenotype as previously thought, but rather are a heterogeneous population with distinct phenotypes and functional characteristics [7]. Therapeutic targeting of the specific fibroblast population responsible for ECM synthesis might be more effective and promising in scar reduction. CD26/dipeptidyl peptidase 4 (DPPIV) is a multifunctional, transmembrane glycoprotein that widely exists on the cell surface in various tissues. A line of evidence has revealed that CD26 is involved in cell adhesion, apoptosis, T cell activation, and immune regulation. The roles of CD26 in skin diseases and its biological effects have become a research hotspot [8]. Through flow sorting and functional validation, this CD26<sup>+</sup> fibroblast subpopulation has been identified as the primary cell type involved in collagen synthesis during skin scar formation and has superior collagen-forming capacity as compared to other subpopulations [9]. Meanwhile, CD26<sup>+</sup> fibroblasts synthesize more collagen during skin wound healing and can induce fibroblast activation in skin fibrotic tissue of TGF- $\beta$ -induced systemic sclerosis [10]. CD26 inactivation interferes with TGF- $\beta$ -induced ERK signaling and reduces the ability of fibroblasts to synthesize collagen [11]. However, oral administration of the CD26 inhibitor linagliptin reduced the expression of inflammatory factors and reduced wound inflammation but increased myofibroblasts in healing wounds of diabetic ob/ob mice [12]. This discrepancy highlights the need to further clarify the role of CD26 during wound healing, especially in specific biological and pathological contexts. Arwert et al found

that the expression of CD26 in dermal tissue increased significantly, while its expression in the tumor stroma decreased during wound-induced skin tumorigenesis in InvEE transgenic mice. Importantly, the use of sitagliptin (an CD26 inhibitor) delayed InvEE tumor growth, while combined treatment with sitagliptin and Kineret (an IL-1 $\alpha$  inhibitor) reduced tumor incidence and delayed tumor formation [13]. Moreover, CD26 inhibitors can significantly inhibit TGF- $\beta$ -induced profibrotic effects, thus suggesting that inhibition of CD26 may be a promising treatment for fibrotic skin diseases [14].

Given that CD26<sup>+</sup> fibroblasts are the predominant subpopulation of fibroblasts involved in collagen biosynthesis and wound healing, this study evaluated the feasibility and effectiveness of CD26 as a potential target for scar reduction using sitagliptin to achieve anti-scarring effects against this specific fibroblast subpopulation.

## Material and Methods

### Skin Wounding Models and Chemical Treatments

The mouse models of both excisional and burn wound healing were utilized to investigate the expression patterns and functions of CD26 during wound healing and scar formation. These models were established as in previous reports, with minor modifications [15]. In total, 15 C57/B6 mice (4-6 weeks old) were divided into 3 groups: normal, excisional, and burn wound healing models, and each individual mouse was administered only 1 treatment. The mice were left to familiarize themselves with the housing facility for 1 week before experiments. The anesthesia method used here was 3% chloral hydrate intraperitoneal injection. I. Excisional wound model: After anesthetization and hair removal of C57/B6 mice, a tissue punch (8 mm in diameter) was used to make 2 symmetrical full-thickness wounds along the dorsal midline. To avoid skin wound contracture, silicone splints (8 mm aperture) were fixed at the edge of the wound using stitches after skin excision. II. Burn wound model: After anesthesia and back hair removal, a customized iron rod with a diameter of 10 mm was preheated for 10 min in a 100°C water bath. Then, the rod was contacted directly on the back skin for 10 s. The wound samples were harvested on days 7, 14, and 21 and further processed for gene expression assays and histopathologic analyses. All animal experiments were reviewed and approved by the Ethics and Research Committee of Nanjing Medical University and conformed to the guidelines of the Institutional Ethics Committee.

### Chemical Treatments In Vivo

A burn skin wound model was used to measure CD26 expression during wound healing and determine the scar-reducing

effects induced by chemically targeting CD26 in vivo. C57/B6 mice (4-6 weeks old) were randomly divided into 3 groups (n=5 per group) as follows: I. Control group, II. Burn wound group, III. Sitagliptin-treated group. I. Control group: Mice were without any treatment. II. Burn wound group: The burn wound group comprised mice with wounds 8 mm in length obtained after the procedure, similar to previous reports [15]. The procedure was as follows: after anesthesia and back hair removal, a customized iron rod with a diameter of 10 mm was preheated for 10 min in a 100°C water bath. Then, the rod was contacted directly on the back skin for 10 s. As a burn wound group, no treatment was given to the wound after scalding until sacrifice at the prescribed time. III. Sitagliptin-treated group: Sitagliptin (10 mg/kg, S5079, Selleckchem, Houston, USA) was administered subcutaneously around the wound edges after burn injury at 24-h intervals and continued until sacrifice. The first dose was immediately administered post-burn, and the final dose was given 1 h before tissue collection. Tissue samples were harvested on day 14 and stored at -80°C until further gene expression quantification and histopathologic analyses were performed.

#### Isolation and Culture of Normal and Wound Fibroblasts and Chemicals Treatment

Primary dermal fibroblasts were isolated from 4-6-week-old naive unwounded and wound healing C57/B6 mice. Normal and wounded skin sections were placed in 0.5% Dispase II (Roche) at 4°C overnight to remove the epidermis. Then, the dermis was cut into small pieces by sharp scissors and cultured in DMEM/F12 (Dulbecco's modified Eagle's medium/F12) containing 10% fetal bovine serum (FBS, Gibco, USA) and antibiotics (penicillin 100 U/ml, streptomycin 100 U/ml, Gibco, USA) at 37°C in a humidified incubator with 5% CO<sub>2</sub>. Migrated fibroblasts from skin explants expanded to 70% confluency and were passaged using trypsin (Invitrogen). Early passage fibroblasts (passages 2-6) were used for all experiments. Sitagliptin (20 nM) was used to pretreat fibroblasts for 24 h after 12 h of starvation with serum-free DMEM/F12. Then, these fibroblasts were used for proliferation, apoptosis, and migration assays.

#### Flow Cytometry for Cell Sorting

FITC anti-mouse CD26 (559652, BD Pharmingen) antibody was used to perform flow cytometry assays to measure the abundance of CD26<sup>+</sup> fibroblast subsets and isolate CD26<sup>+</sup>/CD26<sup>-</sup> fibroblast subpopulations from intact skin (NFs) and wounded skin (WFs). For fluorescence-activated cell sorting (FACS), according to the manufacturer's instructions (FACS Aria II SORP, BD Biosciences), the isolated dermal fibroblasts were washed with Hank's balanced salt solution (HBSS). Then, the cells were washed with buffer (PBS+2% FBS) and incubated with FITC anti-mouse CD26 antibody on ice for 1 h in the dark. The

stained cells were analyzed by FACS with 488 nm excitation, and green fluorescence emission was measured after the incubation period. At least 10 000 events were recorded per sample. The cell populations of both NFs and WF were separated into 4 groups: CD26<sup>+</sup> NFs, CD26<sup>-</sup> NFs, CD26<sup>+</sup> WF, and CD26<sup>-</sup> WF. FACS-sorted cells were collected for further experiments.

#### Cell Proliferation and Apoptosis Assays

Cell proliferation was determined by CCK-8 cell viability assay (Cell Counting Kit-8, Dojindo, Japan). According to the manufacturer's instructions, approximately 3×10<sup>3</sup> cells/well were inoculated into 96-well plates and then cultured in medium containing 10% CCK-8 reaction solution. Two hours later, absorbance was measured at a wavelength of 450 nm by a spectrophotometer plate reader (Multiskan MK3, Thermo). Cell apoptosis was determined by flow cytometry analysis. Additionally, the cells were trypsinized and resuspended in single-cell suspensions. Then, the cells were stained with an Annexin V: PI Apoptosis Detection Kit (BD Bioscience) and detected by a FACS Calibur flow cytometer (BD Biosciences). Data were analyzed using FlowJo analysis software.

#### Cell Migration Assays

Cell migration assays were performed using 2 methods – wound healing and transwell assays – as previously reported [16]. For wound healing assays, approximately 1×10<sup>6</sup> cells/well were inoculated in 6-well plates. An artificial wound was then formed on the confluent cell monolayer with the tip of a sterile 10-μl pipette. The suspended cells were thoroughly rinsed with PBS, cultured in DMEM/F12 with 1% FBS for 0, 6, and 12 h and photographed. For the transwell assay, 1×10<sup>5</sup> viable cells were suspended in 200 μl of serum-free DMEM/F12 medium and inoculated into the upper chamber. Then, complete medium containing 10% serum was added to the lower chamber. After 12-h incubation, a cotton swab was used to gently remove unigrated cells, while the underside of the membrane was stained with a 0.1% crystal violet solution. Images were taken, and the number of migrated cells was calculated.

#### RNA Isolation and Real-time Quantitative PCR

Trizol reagent (Invitrogen) was used to extract total RNA from fresh tissue, and the PrimeScript™ RT-PCR kit (Takara) was used for reverse transcription and PCRs [17]. Detailed gene-specific primers for CD26 and collagen I (Col1) are listed as follows: CD26 (forward: AGTCGCAAACTTACTACTAACTG, reverse: GAGCTGTTCCATATTCAGCATTG) and Col1 (forward: TCTGCGACAACGGCAAGGTG, reverse: GACGCCGGTGGTTCTTGGT). Relative mRNA expressions were quantified and compared with the internal control (GAPDH) by the comparative CT method.

### Protein Extraction and Western Blotting Assay

Cells were collected and lysed with ice-cold RIPA lysis buffer containing protease inhibitor cocktail (Roche, Germany). The lysates were separated by SDS-PAGE and then transferred onto PVDF membranes (Bio-Rad). After blocking with 5% BSA, the membranes were incubated with primary antibodies against CD26 (1: 1000, ab187048, Abcam), Col1 (1: 500, sc-8784, Santa Cruz), and GAPDH (1: 2000, #2118, CST) overnight at 4°C. After incubation of the membranes with horseradish peroxidase (HRP)-conjugated secondary antibodies (Santa Cruz), the blots were finally visualized by enhanced chemiluminescence (Bio-Rad).

### ELISA

After FACS sorting, NFs and WFs were separated into 4 groups – CD26<sup>+</sup> NFs, CD26<sup>-</sup> NFs, CD26<sup>+</sup> WFs, and CD26<sup>-</sup> WFs – and collected for further culture. CD26<sup>+</sup> NFs, CD26<sup>-</sup> NFs, CD26<sup>+</sup> WFs, and CD26<sup>-</sup> WFs were incubated in fibroblast complete medium to 80% confluency and then prepared with serum-free culture medium for 12 h. The released CD26 and Col1 proteins from CD26<sup>+</sup> NFs, CD26<sup>-</sup> NFs, CD26<sup>+</sup> WFs, and CD26<sup>-</sup> WFs were measured using a CD26 ELISA Kit (Abcam, ab264630) and COL1 ELISA Kit (Biovision, E4618-100) according to the manufacturer's instructions. All assays were performed in triplicate and repeated in 3 cell samples.

### Immunofluorescence Staining

Cells were inoculated on glass coverslips, fixed with 4% paraformaldehyde, and washed with PBS. Cells were blocked with 3% BSA for 30 min at room temperature and then incubated with a primary antibody against CD26 (1: 1000, ab187048, Abcam) overnight. Subsequently, the cells were incubated with the secondary antibody and DAPI nuclear staining. A confocal microscope or Zeiss fluorescence microscope was used to observe the immunofluorescence and for photography.

### Histologic and Immunohistochemical Staining

Normal and wounded mouse skin tissues were harvested and fixed overnight with 4% paraformaldehyde. Then, the tissue was washed, dehydrated, and embedded in paraffin. Next, 4- $\mu$ m tissue sections were prepared for Masson trichrome staining (Sigma-Aldrich) and immunohistochemical staining (IHC) according to well-established protocols. Masson trichrome staining was used to analyze total collagen accumulation according to the manufacturer's instructions. For IHC staining, after deparaffinization, rehydration, and antigen retrieval (sodium citrate buffer, pH 6.0), the samples were incubated with CD26 primary antibody (1: 1000, ab187048, Abcam) and corresponding secondary antibodies (Maxim, China) as described

previously [15]. The negative controls group underwent incubation without primary CD26 antibody.

### Statistical Analysis

Quantitative data are presented as the mean $\pm$ SD from 3 independent experiments and were analyzed by *t* test or ANOVA, as appropriate. To confirm the reproducibility and reliability, all independent in vitro experiments were performed in triplicate. *P* values less than 0.05 (2-sided) were considered statistically significant. All statistical analyses were performed using GraphPad Prism 7 (GraphPad Software) and SPSS 22.0 (IBM).

## Results

### Expression Patterns of CD26 in Wounded and Intact Skin

Previous reports have provided clues that CD26 plays critical roles in collagen synthesis and deposition during skin wound healing and organ fibrosis [9,18]. To substantiate the roles of CD26 in skin wound healing, we initially measured the expression patterns of CD26 in both excisional wounds and burn wounds compared with intact skin. As shown in **Figure 1A, 1B**, immunohistochemical staining of samples revealed that CD26<sup>+</sup> cells in both excisional and burn wounds gradually increased, with a peak at postoperative day 14. Consistently, as shown in **Figure 1C, 1D**, remarkable upregulations of CD26 and Col1 at the mRNA level were observed in both excisional and burn wounds, especially at postoperative day 14. Prior studies have identified CD26 as a marker for a specific fibroblast subpopulation in the mouse dermis and its aberrant upregulation in burn wound keloids [9,10,18]. We next sought to examine the proportions of CD26<sup>+</sup> fibroblasts in burn wounds. Through flow cytometric analyses, we found that 48.0% ( $\pm$ 5.8%) of fibroblasts in wounds were CD26<sup>+</sup>, whereas only 29.7% ( $\pm$ 8.3%) of fibroblasts in intact skin were CD26<sup>+</sup>. Together, these results validated that CD26<sup>+</sup> fibroblasts are critically involved in skin wound healing and that their upregulation can contribute to scar formation (**Figure 1E**).

### CD26 Promotes Collagen Biosynthesis, Cell Proliferation, and Migration In Vitro

Considering that our results suggested a profibrogenic role of CD26 in collagen biosynthesis during skin wound healing, we proceeded to delineate the functional differences among 4 fibroblast subpopulations sorted from intact skin (CD26<sup>+</sup> NFs and CD26<sup>-</sup> NFs) and wounds (CD26<sup>+</sup> WFs and CD26<sup>-</sup> WFs) by comparing their capacities for cell proliferation, migration, and collagen biosynthesis. As expected, the results from the CCK-8 assay showed that WFs proliferated faster than NFs. Importantly, the proliferation rate of CD26<sup>+</sup> fibroblasts was

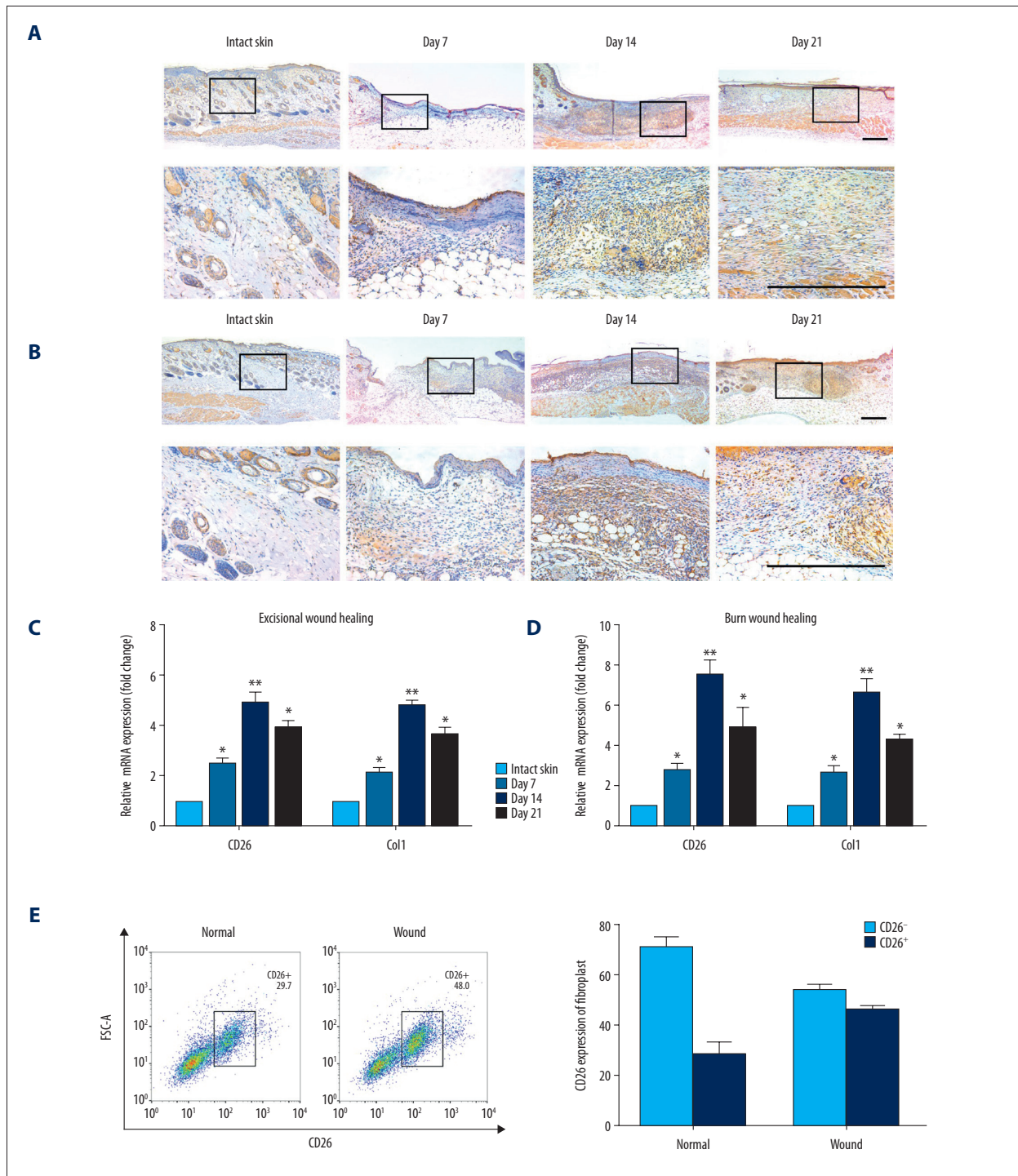


**Figure 1.** Patterns of CD26 Expression in Intact Normal Skin and Skin Wound Models. **(A)** Immunohistochemical staining of CD26 in samples of excisional wounds on days 7, 14 and 21. The **lower panel** corresponds to the high magnification area in the **upper panel**. **(B)** Immunohistochemical staining of CD26 in burn wound samples on days 7, 14, and 21. The **lower panel** corresponds to the high magnification area in the **upper panel**. **(C)** The mRNA expression levels of CD26 and Col1 were significantly increased in samples of skin excisional wounds compared with normal skin (n=5). **(D)** The mRNA expression levels of CD26 and Col1 were significantly increased in burn wound samples compared with normal skin (n=5). **(E)** The proportion of CD26<sup>+</sup> fibroblasts was significantly higher in WFs than in NFs (detected by FACS and its quantification) (n=5). Scale bar: 200  $\mu$ m, *t* test, \* *P*<0.05 vs Intact skin group, \*\* *P*<0.01 vs Intact skin group.

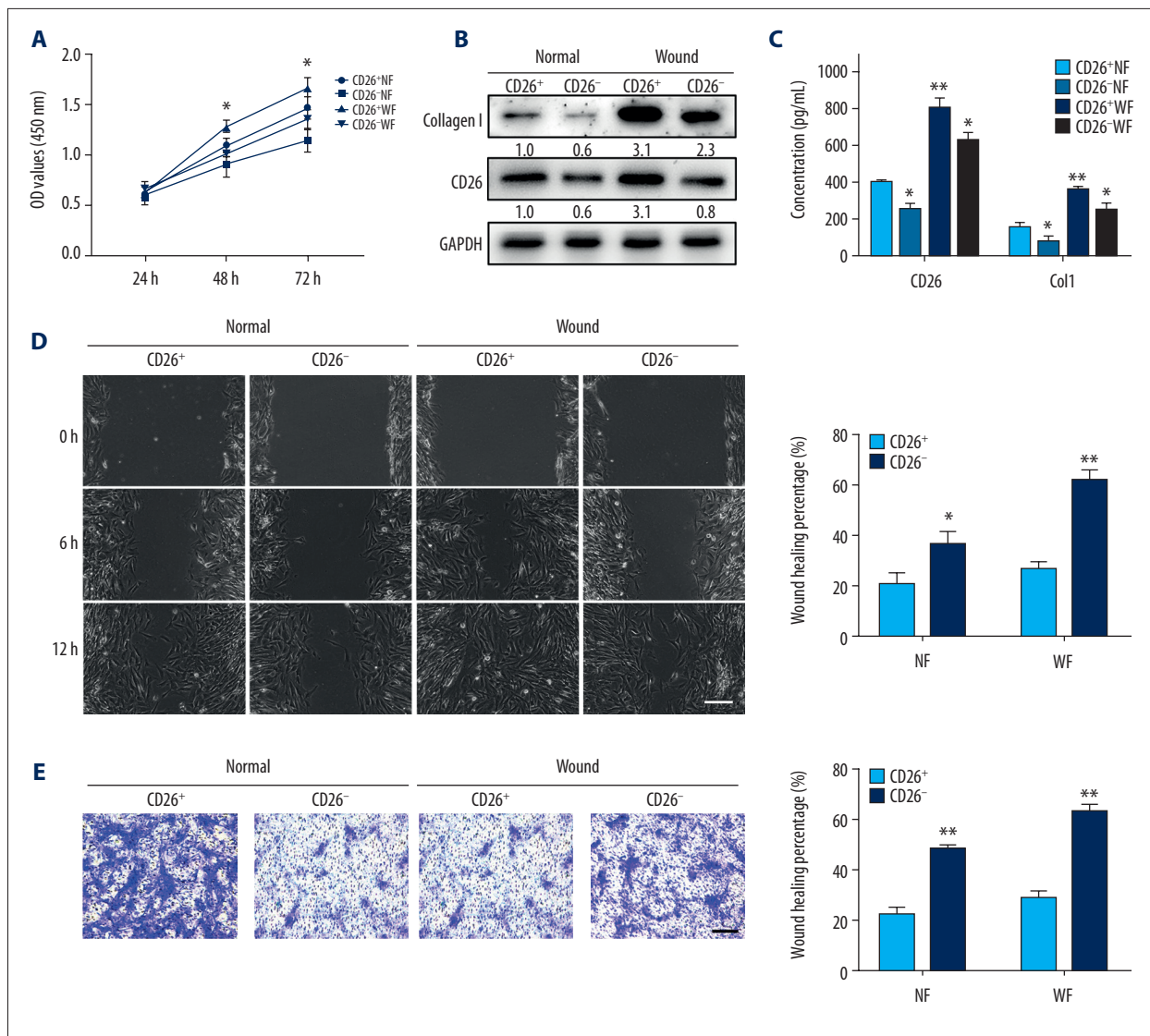


**Figure 2.** CD26 promotes cell proliferation, migration, and collagen biosynthesis in vitro. **(A)** Cell proliferation was remarkably increased in CD26<sup>+</sup> WFs (CCK-8 viability assay). **(B)** The expressions levels of CD26 and Col1 were significantly increased in CD26<sup>+</sup> WFs. Representative images of WB are shown. **(C)** The concentrations of CD26 and Col1 in the supernatant were determined by ELISA (n=5). \*  $P < 0.05$  vs CD26<sup>+</sup> NF group, \*\*  $P < 0.01$  vs CD26<sup>-</sup> NF group. **(D)** Significant enhancement of cell migration in CD26<sup>+</sup> WFs as gauged by wound healing assay and quantification (n=5). \*  $P < 0.05$  vs CD26<sup>-</sup> NF group, \*\*  $P < 0.01$  vs CD26<sup>-</sup> WF group. **(E)** Significant enhancement of cell migration in CD26<sup>+</sup> WFs as gauged by transwell assay and its quantification (n=5). \*\*  $P < 0.01$  vs CD26<sup>-</sup> NF/WF group. Scale bar: 100  $\mu$ m, *t* test.

significantly higher than that of CD26<sup>-</sup> fibroblasts in both NFs and WFs (Figure 2A). To confirm the collagen-promoting biosynthesis role of CD26, the protein abundance of CD26 and Col1 in these 4 subpopulations was measured and compared. Both CD26 and Col1 proteins were significantly enriched in those CD26<sup>+</sup> fibroblasts, especially in CD26<sup>+</sup> WFs (Figure 2B, 2C). The migratory potentials of fibroblasts were measured by wound healing and transwell assays. As shown in Figure 2D, 2E, the migratory abilities of CD26<sup>+</sup> WFs were significantly superior to those of the other 3 subpopulations. Collectively, these results

confirmed that CD26<sup>+</sup> fibroblasts have diverse biological behaviors and phenotypes as compared to CD26<sup>-</sup> fibroblasts and suggest that therapeutic targeting of CD26 during wound healing to reduce scarring warrants further experimental exploration.

#### Sitagliptin Suppresses the Profibrogenic Roles of CD26<sup>+</sup> Fibroblasts In Vitro

Previous pioneering studies clarified a potent CD26-targeting mechanism by sitagliptin and demonstrated its promising

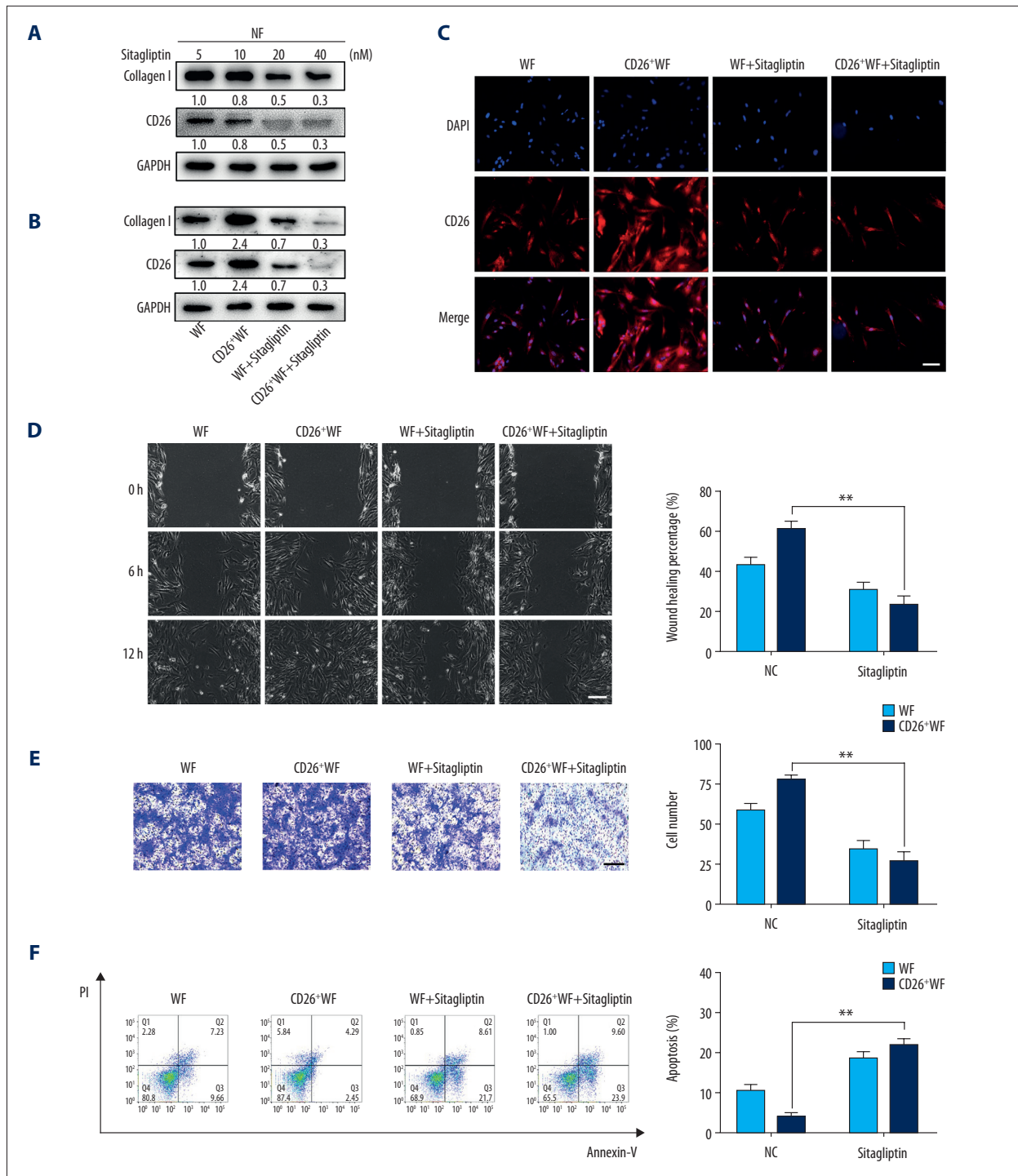


**Figure 3.** Sitagliptin inhibits the pathological features of CD26<sup>+</sup> wound fibroblasts in vitro. **(A)** The expression of CD26 and Col1 in WFs and CD26<sup>+</sup> WFs was measured by western blot following a concentration gradient of sitagliptin treatment. Representative images are shown. **(B)** Immunofluorescent staining of CD26 in WFs and CD26<sup>+</sup> WFs after sitagliptin treatment. Representative images are shown. **(C)** The migration ability of CD26<sup>+</sup> WFs was significantly reduced following sitagliptin treatment (20 nM) in wound healing assays. **(D)** The migration ability of CD26<sup>+</sup> WFs was significantly reduced after sitagliptin treatment (20 nM) in transwell assays. **(E, F)** An evident increase in apoptosis within the WFs and CD26<sup>+</sup> WFs following sitagliptin treatment (20 nM) as assayed by Annexin V-PI staining and its quantification (n=5). Scale bar: 100  $\mu$ m. *t* test, \* *P*<0.05 vs WF group, \*\* *P*<0.01 vs WF group.

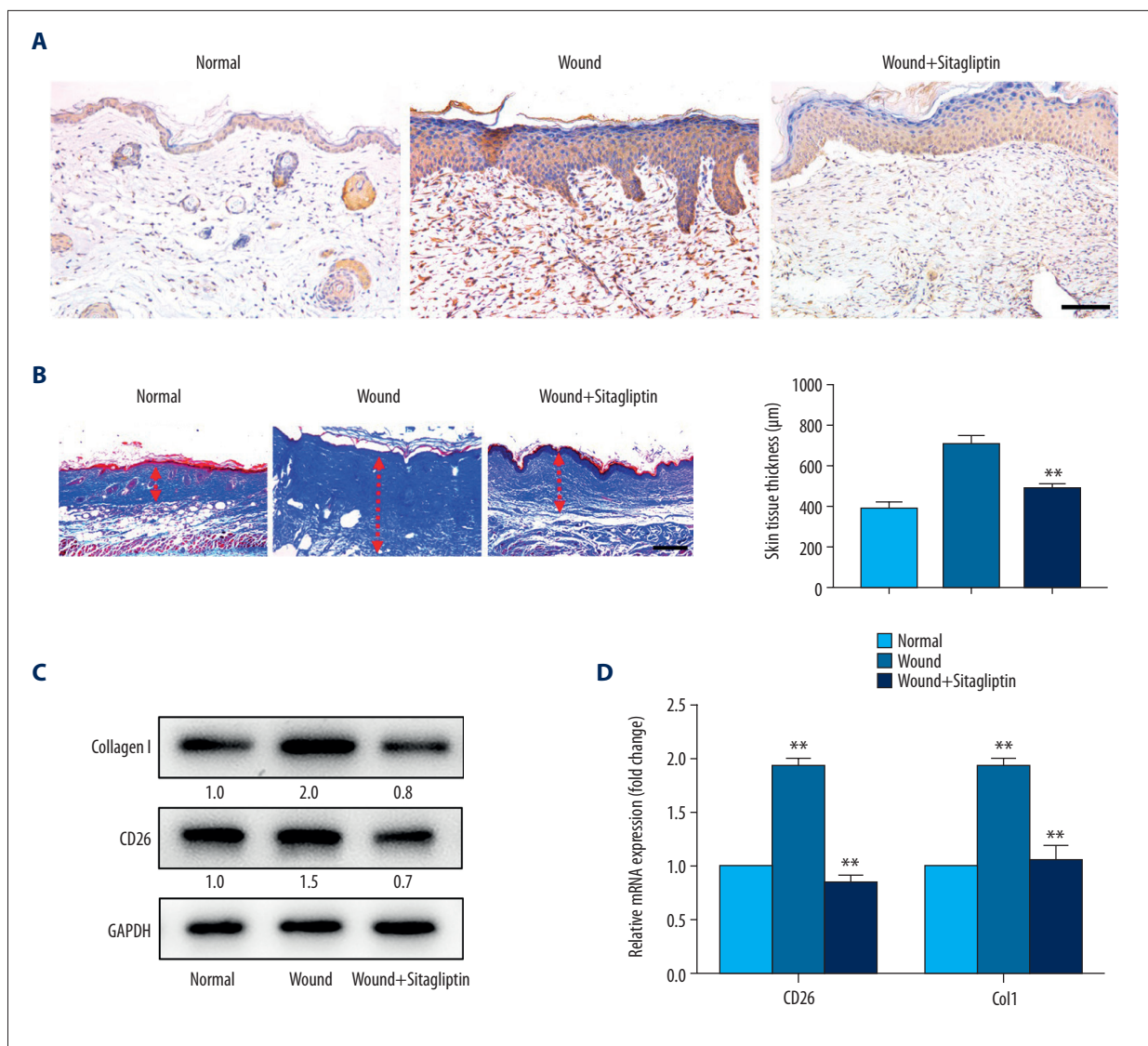


**Figure 4.** Pharmacological inhibition of CD26 inhibits collagen biosynthesis during skin wound healing and reduces scar formation. **(A)** Immunohistochemistry staining of CD26 in samples of normal skin, burn wounds, and wounds treated with sitagliptin. Scale bar: 100 µm. **(B)** Masson staining in samples of normal skin, burn wounds, and wounds treated with sitagliptin and its quantification (n=5). Scale bar: 200 µm. **(C)** The protein expressions levels of CD26 and Col1 in tissue samples following sitagliptin treatment were measured by western blot. Representative images are shown. **(D)** The mRNA expression levels of CD26 and Col1 were significantly decreased in samples of skin burn wounds following sitagliptin treatment (n=5). *t* test, \*  $P < 0.05$  vs Normal group, \*\*  $P < 0.01$  vs Normal group.

function as a single agent against various fibrotic diseases, including kidney fibrosis, systemic sclerosis, and hepatic fibrosis [11,19,20]. Therefore, to verify the therapeutic potentials of sitagliptin in wound healing and scar prevention, we investigated its inhibitory functions *in vitro*. First, we chose a suitable dose of sitagliptin through concentration gradient and identified 20 nM as the appropriate dose (Figure 3A). As expected, sitagliptin exposure induced a remarkable decrease in CD26 and Col1 protein expression in CD26<sup>+</sup> WFs compared to WFs (Figure 3B, 3C). Moreover, as shown in Figure 3D, 3E, the

migratory properties of CD26<sup>+</sup> WFs were significantly impaired after sitagliptin treatment. In addition, an annexin V-PI flow cytometric assay showed a significant increase in the proportions of apoptotic cells in sitagliptin-treated CD26<sup>+</sup> WFs (Figure 3F).

#### Pharmacological Inhibition of CD26 Inhibits Collagen Biosynthesis During Skin Wound Healing

Having revealed the inhibitory properties of sitagliptin by targeting CD26 *in vitro*, we further developed a burn wound



model to establish the treatment effects of sitagliptin *in vivo*. Following burn wound establishment, sitagliptin (10 mg/kg) was injected after burn injury at 24-h intervals and continued until sacrifice on day 14. The dorsal skins of all 3 groups (intact skin, burn wound, and sitagliptin-treated burn wound) were harvested for histopathological analyses for CD26 and Col1 expression. The IHC results revealed lower CD26 staining in samples from sitagliptin-treated wounds than in burn wounds without treatment (**Figure 4A**). In agreement with these results, Masson staining indicated a significant decrease in collagen fibers and a thinner dermal layer at the wound site in sitagliptin-treated wounds than in other wounds (**Figure 4B**). Furthermore, sitagliptin treatment yielded a remarkable decline in the mRNA expressions and protein abundance of CD26 and Col1 in wounds (**Figure 4C, 4D**), suggesting the potential inhibitory effects of sitagliptin on collagen synthesis during the skin wound healing process.

## Discussion

Abnormal synthesis, secretion, and deposition of collagen-dominant ECM during skin wound healing are the main pathological bases of scar formation. Although various cells are involved in collagen synthesis and scar contracture, like fibroblasts and epithelial and adipogenic stem cells, specific skin fibroblast subpopulations have been found to govern extracellular matrix synthesis and scar formation [21]. Indeed, fibroblasts usually presented remarkable differences in morphology, proliferation rate, and synthesis of cytokines and extracellular matrix [22,23]. Here, we utilized both *in vitro* and *in vivo* experiments to confirm the increased CD26<sup>+</sup> fibroblasts during wound healing and revealed potent pro-fibrogenic effects of CD26 in dermal fibroblasts. Pharmacological targeting of CD26 reduced the abundance of fibroblasts and collagen production during skin wound healing.

Initially, CD26 was identified as a type II transmembrane glycoprotein and secreted protein comprising 2 subunits fixed on the cell membrane by N-terminal hydrophilic region, and was involved in signaling pathways to exert various biological effects [8,24]. As an adhesion molecule, CD26 can bind to the collagen and fibronectin and slow the migration of murine hepatocytes in cell matrix [25]. It functions as a lymphocyte extracellular enzyme in regulating nutrient uptake and recycling [26], and as a cell membrane receptor and costimulatory molecule to mediate T cell signal transduction by interacting with adenosine deaminase, CD45, or CARMA1 [27]. Experiments also revealed that in skin transplantation, the deficiency of CD26 inhibited the differentiation of CD4<sup>+</sup> cells into Th1, Th2, and Th17 subsets and instead promotes differentiation into

Tregs, which contribute to immune tolerance after allografting. It is noteworthy that CD26 participates in skin healing in 2 ways: immune regulation and fibroblast regulation during skin transplantation [28]. Of particular interest, Rinkevich et al identified a subgroup of dermal fibroblasts originating from the expression of engrailed-1 (En1) progenitor cells, which are closely related to the formation of skin scarring in early pregnancy. In addition, CD26 could be used as a marker to enrich 94% of En1-positive fibroblasts, further supporting the heterogeneity of the dermal fibroblast population [9]. Together with these findings, our results confirm the key roles of CD26 by serving as a surface marker for specific fibroblast subsets with robust profibrogenic roles and a functional mediator underlying skin wound healing.

Given its roles of CD26 during skin wound healing and scarring, we hypothesized that inhibition of CD26 is a promising treatment strategy for skin fibrotic diseases such as keloids. Our results show that the proliferation and migration rates of CD26<sup>+</sup>WFS cells are higher than those of CD26<sup>+</sup>NFS cells. In line with this, Awert et al also reported that higher wound closure, revascularization, and cell proliferation rates were observed in CD26<sup>-/-</sup> mice [28]. This implies that CD26 regulates multiple aspects of wound healing in addition to fibroblasts and collagen biosynthesis. Noticeably, sitagliptin exerts significant anti-fibrogenic effects and displays tremendous translational potentials [19]. Our results derived from *in vitro* cellular experiments revealed that sitagliptin significantly reduced CD26 and Col1 abundance in CD26<sup>+</sup> fibroblasts, inhibited migration, and promoted cell apoptosis. Moreover, we developed a burn skin wound model and verified that local delivery of sitagliptin markedly inhibited collagen production and thickening of the dermis during wound healing *in vivo*. These findings support the key roles of CD26 during wound healing and offer evidence to support a novel therapeutic strategy by targeting CD26 to reduce skin scar formation. Of course, much work is needed to further delineate the spatiotemporal expressions of CD26 during skin wound healing and scar formation and unravel the detailed mechanisms mediated by CD26 in driving skin scar formation.

## Conclusions

In conclusion, our results reveal that CD26 participates in skin wound healing and scar formation, probably by mediating proliferation, migration, collagen synthesis, and secretion of fibroblasts. These findings provide clues regarding the therapeutic utility of CD26 inhibitor to effectively inhibit scar formation in the future.

## References:

- Broughton G 2<sup>nd</sup>, Janis JE, Attinger CE. The basic science of wound healing. *Plast Reconstr Surg*, 2006;117:125-345
- Rosenbaum AJ, Banerjee S, Rezak KM, Uhl RL. Advances in wound management. *J Am Acad Orthop Surg*, 2018;26:833-43
- Eming SA, Martin P, Tomic-Canic M. Wound repair and regeneration: Mechanisms, signaling, and translation. *Sci Transl Med*, 2014;6:265sr6
- Darby IA, Zakuan N, Billet F, Desmouliere A. The myofibroblast, a key cell in normal and pathological tissue repair. *Cell Mol Life Sci*, 2016;73:1145-57
- Wang YW, Liou NH, Cherng JH, et al. siRNA-targeting transforming growth factor-beta type I receptor reduces wound scarring and extracellular matrix deposition of scar tissue. *J Invest Dermatol*, 2014;134:2016-25
- Hsu I, Parkinson LG, Shen Y, et al. Serpina3n accelerates tissue repair in a diabetic mouse model of delayed wound healing. *Cell Death Dis*, 2014;5:e1458
- Driskell RR, Lichtenberger BM, Hoste E, et al. Distinct fibroblast lineages determine dermal architecture in skin development and repair. *Nature*, 2013;504:277-81
- Lee SA, Kim YR, Yang EJ, et al. CD26/DPP4 levels in peripheral blood and T cells in patients with type 2 diabetes mellitus. *J Clin Endocrinol Metab*, 2013;98:2553-61
- Rinkevich Y, Walmsley GG, Hu MS, et al. Skin fibrosis. Identification and isolation of a dermal lineage with intrinsic fibrogenic potential. *Science*, 2015;348:aaa2151
- Worthen CA, Cui Y, Orringer JS, et al. CD26 identifies a subpopulation of fibroblasts that produce the majority of collagen during wound healing in human skin. *J Invest Dermatol*, 2020;140(12):2515-24.e3
- Soare A, Gyorfi HA, Matei AE, et al. Dipeptidylpeptidase 4 as a marker of activated fibroblasts and a potential target for the treatment of fibrosis in systemic sclerosis. *Arthritis Rheumatol*, 2020;72:137-49
- Schurmann C, Linke A, Engelmann-Pilger K, et al. The dipeptidyl peptidase-4 inhibitor linagliptin attenuates inflammation and accelerates epithelialization in wounds of diabetic ob/ob mice. *J Pharmacol Exp Ther*, 2012;342:71-80
- Arwert EN, Mentink RA, Driskell RR, et al. Upregulation of CD26 expression in epithelial cells and stromal cells during wound-induced skin tumour formation. *Oncogene*, 2012;31:992-1000
- Thielitz A, Vetter RW, Schultze B, et al. Inhibitors of dipeptidyl peptidase IV-like activity mediate antifibrotic effects in normal and keloid-derived skin fibroblasts. *J Invest Dermatol*, 2008;128:855-66
- Zhu Y, Li Z, Wang Y, et al. Overexpression of miR-29b reduces collagen biosynthesis by inhibiting heat shock protein 47 during skin wound healing. *Transl Res*, 2016;178:38-53.e6
- Zhang W, Ge H, Jiang Y. Wound repair and regeneration: Mechanisms, signaling, and translation. Combinational therapeutic targeting of BRD4 and CDK7 synergistically induces anticancer effects in head and neck squamous cell carcinoma. *Cancer Lett*, 2020;469:510-23
- Wu Y, Wang Y, Diao P, et al. Therapeutic targeting of BRD4 in head neck squamous cell carcinoma. *Theranostics*, 2019;9:1777-93
- Tabib T, Morse C, Wang T, et al. SFRP2/DPP4 and FMO1/LSP1 define major fibroblast populations in human skin. *J Invest Dermatol*, 2018;138:802-10
- Liu X, Zhang T, Zhang C. Sitagliptin inhibits extracellular matrix accumulation and proliferation in lung fibroblasts. *Med Sci Monit*, 2020;26:e922644
- Kanasaki K, Shi S, Kanasaki M, et al. Linagliptin-mediated DPP-4 inhibition ameliorates kidney fibrosis in streptozotocin-induced diabetic mice by inhibiting endothelial-to-mesenchymal transition in a therapeutic regimen. *Diabetes*, 2014;63:2120-31
- Driskell RR, Watt FM. Understanding fibroblast heterogeneity in the skin. *Trends Cell Biol*, 2015;25:92-99
- Sorrell JM, Caplan AI. Fibroblast heterogeneity: More than skin deep. *J Cell Sci*, 2004;117:667-75
- Mine S, Fortunel NO, Pigeon H, Asselineau D. Aging alters functionally human dermal papillary fibroblasts but not reticular fibroblasts: A new view of skin morphogenesis and aging. *PLoS One*, 2008;3:e4066
- Boonacker E, Van Noorden CJ. The multifunctional or moonlighting protein CD26/DPP4. *Eur J Cell Biol*, 2003;82:53-73
- Hanski C, Huhle T, Reutter W. Involvement of plasma membrane dipeptidyl peptidase IV in fibronectin-mediated adhesion of cells on collagen. *Biol Chem Hoppe Seyler*, 1985;366:1169-76
- Klemann C, Wagne L, Stephan M, von Horsten S. Cut to the chase: A review of CD26/dipeptidyl peptidase-4's (DPP4) entanglement in the immune system. *Clin Exp Immunol*, 2016;185:1-21
- Ohnuma K, Dang NH, Morimoto C. Revisiting an old acquaintance: CD26 and its molecular mechanisms in T cell function. *Trends Immunol*, 2008;29:295-301
- Zhao X, Zhang K, Daniel P, et al. Delayed allogeneic skin graft rejection in CD26-deficient mice. *Cell Mol Immunol*, 2019;16:557-67